

Influence of the Circulating Current on the Propagation of the Change in Membrane Potential

Yuki KUSHIDA, Osamu SHIRAI,[†] Yoshinari TAKANO, Yuki KITAZUMI, and Kenji KANO

Division of Applied Life Sciences, Graduate School of Agriculture, Kyoto University, Sakyo, Kyoto 606-8502, Japan

The propagation of the change in potential differences across liquid membranes from the potential-sending cell to the potential-receiving cell was investigated by use of a system combined with three liquid membrane cells, which were composed of two aqueous phases and a 1,2-dichloroethane solution phase. The ionic composition of one potential-sending cell (S) was identical to that of the receiving cell (Rec), and that of another potential-sending cell (Ap) was different from that of the Rec. When the connection of cell Rec was switched from cell S to cell Ap, the change in the membrane potential was caused by the circulating current. The greater the ratio of the interfacial area of the membrane of cell Ap to that of cell Rec, the faster the change in the membrane potential propagated from cell Ap to cell Rec.

Keywords Liquid membrane, membrane potential, ion transport, propagation, circulating current, potentiometry

(Received February 24, 2015; Accepted April 29, 2015; Published July 10, 2015)

Introduction

The membrane potential of a nerve cell is usually determined by the ratio of the inside K^+ concentration to that of the outside and is called the rest potential.¹⁻⁶ When neurotransmitters bind to a specific channel-type receptor at the synapse, Na^+ is mainly transported from the outside to the inside by opening the channels. When the current due to the transport of Na^+ from the outside to the inside exceeds the threshold, the membrane potential changes from the rest potential to the action potential regulated by the ratio of the inside Na^+ concentration to that of the outside. The change in the membrane potential is successively propagated along the axon by opening the voltage-gated Na^+ channels of which the open-times are short (about 1 ms).⁷ Thus, the action potential is propagated along the axon toward the axon terminal. At the same time, K^+ is transported from the inside to the outside of the nerve cell by opening the delayed K^+ channels to maintain the electroneutrality of every phase. Accordingly, it is generally considered that the membrane potential is determined by the transport of two ion species (K^+ and Na^+). Although the direction of the propagation is explained by the channel properties, such as the open lifetime and deactivation, it is difficult to elucidate the direction of the propagation from the mitral cell dendrites to the synapse terminals.¹⁻³ On the other hand, it is well-known that the area of the mitral cell dendrites is still larger than that of the synapse terminals.¹ This structure seems to be adequate for rapid conduction because the influx of Na^+ increases with an increase in the area of the mitral cell dendrites. The relation between the propagation properties of the action potential and the area ratio of the membrane site at the action potential to that at the rest

potential has not been elucidated.

Our group has proposed a new propagation mechanism for the change in the membrane potential using a U-shaped organic liquid membrane cell system.^{8,9} We successfully reproduced the propagation of the action potential by regulating the transport of two ion species and found the electrochemical meaning of the threshold and the local propagation mechanism. Taking into account the electroneutrality principle and the mass balance of electrolyte ions in every phase, the propagation of the action potential is caused by the generation of the circulating current between the sending and receiving sites.^{9,10} On the other hand, it has been reported that the decrease and/or the delay in the propagation of the action potential are ascribed to the charging current at the membrane surface and to the ohmic drop due to the solution resistance,¹¹⁻¹⁷ and we interpreted the influence of the charging current and the ohmic drop on the propagation of the change in the membrane potential using some capacitors and resistors within the electric circuit.¹⁰ However, the influence of the direction on the propagation of the action potential and the magnitude of the circulating current has not yet been explained.

In the present study, the influence of the ratio of the area of the potential-sending site to that of the potential-receiving site on the propagation of the action potential is elucidated by use of liquid membrane cells with different membrane areas.

Experimental

Reagents and chemicals

Sodium tetrakis[3,5-bis(trifluoromethyl)phenyl]borate (NaTFPB) was produced in a manner similar to that previously reported.¹⁸ The TFPB⁻ salts of bis(triphenylphosphoranylidene)ammonium (BTTPATFPB) and tetraethylammonium (TEATFPB) were obtained by mixing a methanol solution of NaTFPB with a methanol solution of BTTPACl (Sigma-Aldrich Co.) and TEACl

[†] To whom correspondence should be addressed.
E-mail: shirai@kais.kyoto-u.ac.jp

(Wako Pure Chemical Industries, Inc.), respectively, as previously described.¹⁸ The precipitates of BTPPATFPB and TEATFPB were separately purified by recrystallization based on the temperature dependence of the solubility of the salts in ethanol. After these salts were dissolved in 1,2-dichloroethane (DCE), the DCE solution was mixed with pure water, then separated to remove any impurities. The residual current due to the impurities was less than 10 nA and it did not affect the results.

All other chemicals were of analytical reagent grade and were used without further purification.

Apparatus

The potentiometric measurements were carried out using an HA-1010 mM4A (Hokuto Denko Co.) potentiostat/galvanostat and an A/D converter Model GL900 (Graphtec Co.). The circulating current was measured by an HM-103 ammeter (Hokuto Denko Co.). The collection data were recorded every 5 ms. A rotary switch M43 (Alps Electric Co.) was set up within the electric circuit, as shown in Fig. 1(a).

Electrochemical measurements

The cell system combined with three liquid-membrane cells, which were composed of two aqueous phases (W1 and W2) and a DCE phase, respectively, is illustrated in Fig. 1. The propagation of the change in the potential difference across the liquid membrane (M) from the sending-site to the receiving-site was evaluated. The respective W1 (and W2) phases of the three cells were electrically connected by lead wires to Ag|AgCl electrodes. The ionic composition of one potential-sending cell (S) and two potential-receiving cells (Rec and rec) were noted by Eq. (1).

W1	M	W2
0.1 M NaCl	10 ⁻³ M TEATFPB	5 × 10 ⁻³ M TEACl
3% agar	10 ⁻⁵ M NaTFPB	0.1 M NaCl
(RE1)	10 ⁻² M BTPPATFPB	3% agar
	(RE2, RE3)	(RE4)

(1)

The cell configuration of the two potential-sending cells (Ap and ap) is then represented by Eq. (2).

W1	M	W2
2 × 10 ⁻⁵ M TEACl	10 ⁻³ M TEATFPB	5 × 10 ⁻³ M TEACl
0.1 M NaCl	10 ⁻⁵ M NaTFPB	0.1 M NaCl
3% agar	10 ⁻² M BTPPATFPB	3% agar
(RE1)	(RE5)	(RE4)

(2)

where the membrane area of cell S, Ap or Rec was 1.33 cm², and that of cell ap or rec was 0.331 cm². Although the nerve conduction is determined by the transport of K⁺ and Na⁺, the membrane potential in the present system was determined by the transport of Na⁺ and TEA⁺. Since the difference between the standard ion transfer potential of K⁺ and that of Na⁺ is still less than 0.1 V, it is difficult to analyze the ion transfer reaction at the interfaces between the W and DCE.¹⁹ Accordingly, the authors selected Na⁺ and TEA⁺ as the transporting ions because the standard ion transfer potential of Na⁺ is more than 0.5 V higher than that of TEA⁺. The influence of the ratio of the area of the potential-sending site to that of the potential-receiving site on the propagation of the change in the membrane potential was investigated by considering the structure of the nerve cells. The membrane phase, which consisted of DCE (2 mL each)

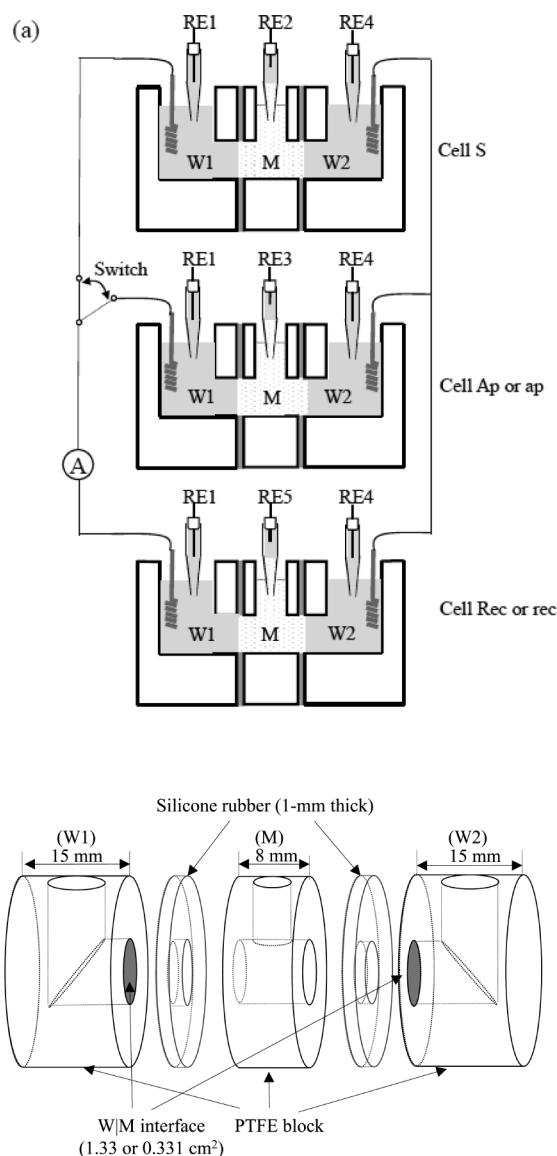


Fig. 1 Cell system composed of three liquid membrane cells (S, Rec, rec, Ap and ap) (a) and construction of each cell (b). Sending site: cells S, Ap and ap; receiving site: cells Rec and rec. W (W1 and W2); aqueous phases, M; liquid membrane (DCE). Interfacial area: 1.33 cm² (S, Ap and Rec), 0.331 cm² (ap and rec). RE1-5; reference electrodes.

containing 10⁻² M BTPPATFPB as a supporting electrolyte to lower the solution resistance in M, was placed between W1 (3 mL) and W2 (3 mL). The electric resistance of each cell was about 500 Ω. Each of the six Ag|AgCl electrodes (RE1 and RE4) was immersed in W1 and W2 of every cell, and three TEA⁺ selective electrodes (TEA-ISE: RE2, RE3 and RE5) were immersed in M of every cell.²⁰ Equation (3) indicates the cell configuration of the TEA-ISE.



The respective W1 (and W2) phases of the three cells were electrically connected to each other by lead wires to Ag|AgCl electrodes in order not to generate a potential difference between W1 (W2) of the potential-sending cells and W1 (W2) of the potential-receiving cell. Accordingly, the reference electrodes in W1 and W2 of each cell were described as RE1 and RE4,

respectively. The potential differences at the W1|M and W2|M interfaces ($E_{W1|M}$ and $E_{W2|M}$) of all cells were represented as the potentials of RE1 and RE4 vs. the TEA-ISE of each cell. Since W1, W2 and M of each cell contained a sufficient amount of electrolyte, the potential drop due to the solution resistance was less than 1 mV at 1 μ A. Therefore, the potential difference between W1 and W2 (E_{W1-W2}) can be expressed by both $E_{W1|M}$ and $E_{W2|M}$, as given below.

$$E_{W1-W2} = E_{W1|M} - E_{W2|M} \quad (4)$$

First, the potential-receiving cell (Rec or rec) was connected to the potential-sending cell (S). When the connection of the cell Rec or rec was switched from cell S to cell Ap or ap by using a rotary switch, the changes in E_{W1-W2} , $E_{W1|M}$ and $E_{W2|M}$ of cells S, Ap, ap, Rec and rec ($E_{W1-W2, S}$, $E_{W1|M, S}$, $E_{W2|M, S}$, $E_{W1-W2, Ap}$, $E_{W1|M, Ap}$, $E_{W2|M, Ap}$, $E_{W1-W2, ap}$, $E_{W1|M, ap}$, $E_{W2|M, ap}$, $E_{W1-W2, Rec}$, $E_{W1|M, Rec}$, $E_{W2|M, Rec}$, $E_{W1-W2, rec}$, $E_{W1|M, rec}$, $E_{W2|M, rec}$) were measured and the circulating current was also simultaneously recorded.

Results and Discussion

The propagation of the change in the membrane potential caused by the circulating current

Figure 2(a) indicates the time-courses of $E_{W1|M, Rec}$ and $E_{W1|M, Ap}$, of which the current between W1 and W2 was 0 A. After the connection of cell Rec was switched from cell S to cell Ap, the circulating current was generated, as shown in Fig. 2(b), and $E_{W1|M, Rec}$ and $E_{W1|M, Ap}$ were changed. Similarly, $E_{W1-W2, Ap}$ and $E_{W1-W2, Rec}$ were changed from 0.16 and 0.37 V to 0.25 and 0.25 V, respectively. Although the current was not observed at each interface before the switching, the current flowed at each interface after the switching.

Figure 3 indicates the imaginary steady-state voltammograms for the ion transfer between W1 and DCE (M) by considering the transfer energies of Na^+ and TEA^+ from W to DCE (0.591 and 0.019 V vs. TPhE, respectively) and the ion composition of the present cell system.¹⁹ Here, TPhE indicates the standard potential, which is a midpoint potential between the standard potential, for the transfer of tetraphenylborate and that of tetraphenylarsonium. In the present case, the current due to the transfer of other ions was not practically observed. In this figure, the potential difference between W1 and M (DCE) is represented for TEAE, which is defined by regarding the potential difference for the transfer of TEA^+ between W and DCE as 0 V. Although the positive current is attributed to both the transfer of a cation (Na^+ or TEA^+) from W1 to M (DCE) and that of an anion from M (DCE) to W based on the definition of voltammetry for the ion transfer between two immiscible electrolyte solutions, the potential difference and the current of the imaginary voltammograms at the W2|M interface are reversed by considering the direction of the ion transport between W1 and W2 ($E_{M|W2} = -E_{W2|M}$, $i = -i_{W2|M}$). Figure 3 shows the imaginary steady-state voltammograms at the W1|M interfaces of cells Ap and Rec, when cell Ap is connected to cell Rec. In the present case, the potential window of the imaginary voltammogram at every W|M interface is determined by both the transport of Na^+ from W to DCE and that of TEA^+ from DCE to W. The ion transfer current clearly flows within the potential window between 0.05 V and 0.45 V in the presence of Na^+ in DCE (negative current) or TEA^+ in W (positive current). On the other hand, the W2|M interface of each cell was depolarized by the transfer of TEA^+ , and the $E_{W2|M}$ of each cell was almost constant (-0.10 V) regardless of the connection.

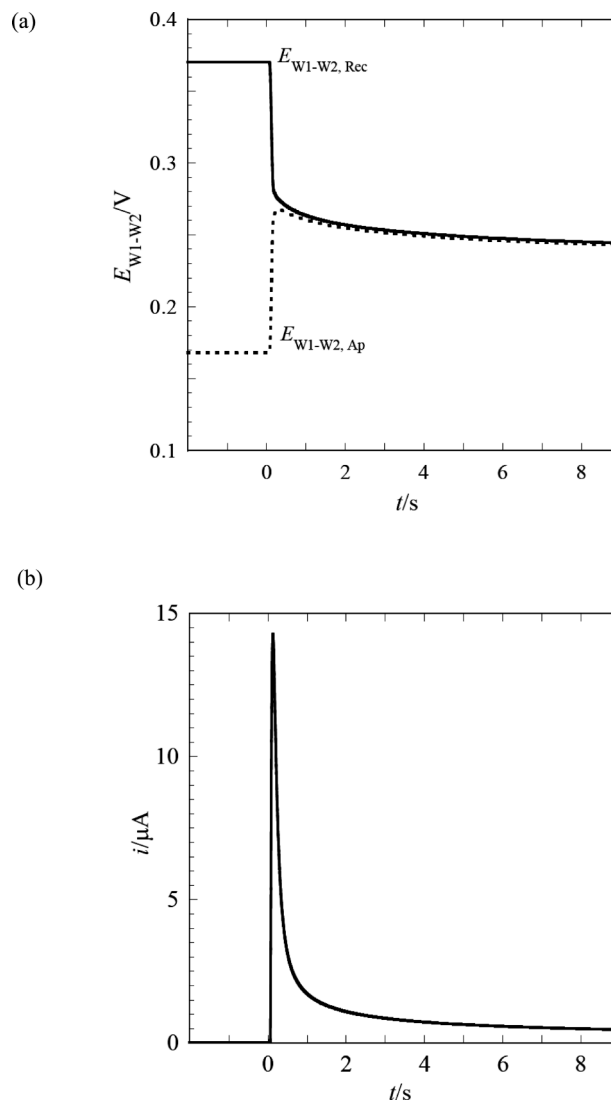


Fig. 2 The time-courses of the membrane potentials of potential-receiving and potential-sending cells ($E_{W1-W2, Rec}$ and $E_{W1-W2, Ap}$) by changing the connection with cell Rec from cell S to cell Ap (a) and the circulating current (i) (b). $t = 0$: the period of the switch. Interfacial area: 1.33 cm² (S, Ap and Rec).

Accordingly, the change in E_{W1-W2} was almost equal to that in $E_{W1|M}$. Before the switch, $E_{W1|M}$ of cell Rec was determined by the transfer of Na^+ (closed diamond). Since the W1|M interface of cell Ap was depolarized by the transfer of TEA^+ , $E_{W1|M}$ of cell Ap was 0.06 V before the switch. After connection of cell Rec was changed from cell S to cell Ap, the $E_{W1|M}$ of cell Rec was shifted in the negative direction (closed circle) with any circulating current.

Influence of the area ratio of the potential-sending site to the potential-receiving site on propagation of the change in the membrane potential

Figure 4(a) indicates the time-courses of $E_{W1-W2, Rec}$ and $E_{W1-W2, rec}$ when the connection was changed from cell S to cell Ap or ap. The time-courses of $E_{W1-W2, Ap}$ and $E_{W1-W2, ap}$ were observed at the same time, as shown in Fig. 4(b). The circulating current was generated after the switch, as represented in Fig. 4(c). The $E_{W1|M}$ values changed at the same time. When the connection of cell rec was switched from cell S to cell Ap,

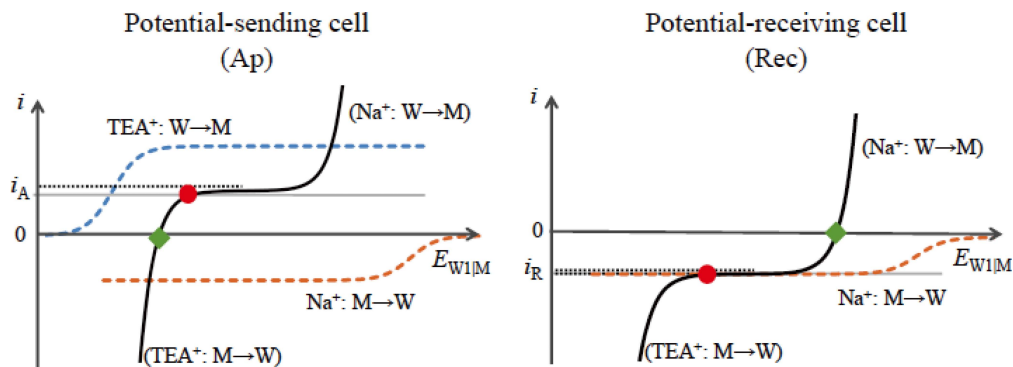


Fig. 3 Schematic steady-state voltammograms by considering the ionic composition and the ion transfer potentials of the ions at the interfaces of W1|M of cells Ap and Rec.¹⁹ ◆: $E_{W1M, Ap}$ and $E_{W1M, Rec}$ observed before the switch, ●: $E_{W1M, Ap}$ and $E_{W1M, Rec}$ observed after the switch. Gray line: the circulating current. Interfacial area: 1.33 cm² (S, Ap and Rec).

the change in the membrane potential of the potential-receiving cell was the highest and approached 0.18 V which was close to the initial action potential (the $E_{W1-W2, Ap}$ value observed before the switch). On the contrary, the change in the membrane potential of the potential-receiving cell was the lowest when cell Rec was connected with cell ap. The circulating current was the highest when cell Rec was connected to cell Ap (Ap-Rec connection), and the current 8 s after the switch was about 0.50 μ A, as represented by Fig. 2(b). The change in the membrane potential of cell rec by connecting to cell ap (ap-rec connection) was equivalent to that obtained in the case of the connection of cell Ap with cell Rec. However, the circulating current was the lowest and the current 8 s after the switching was about 0.15 μ A. Since the current density of the circulating current of cell Ap (or Rec) is identical to that of cell ap (or rec), it is clear that the magnitude of the circulating current is proportional to the membrane area and that the change in the membrane potential of the Ap-Rec connection is equivalent to that of the ap-rec connection. Thus, it is important for the propagation of the change in the membrane potential to have the ability to generate a higher electric charge at the potential-sending site.

Figures 5(a) – 5(c) indicate the imaginary voltammograms at the W1|M interfaces of the potential-sending and the potential-receiving cells (ap-rec, Ap-rec and ap-Rec connections), respectively. In the present case, the potential window of the imaginary voltammogram at every W1|M interface is determined by both the transport of Na⁺ from W to DCE and that of TEA⁺ from DCE to W. The ion transfer current clearly flows within the potential window between 0.05 and 0.45 V in the presence of Na⁺ in DCE (negative current) or TEA⁺ in W (positive current). Since the ionic composition of cells Rec and rec is identical to that of cell S, $E_{W1M, S}$ and $E_{W2M, S}$ are equivalent to $E_{W1M, Rec}$ and $E_{W2M, Rec}$ ($E_{W1M, rec}$ and $E_{W2M, rec}$), respectively, before the switch. These are illustrated by the closed diamonds in Fig. 5. Incidentally, $E_{W1M, S}$, $E_{W1M, Rec}$ and $E_{W1M, rec}$ observed before the switch are governed by the distribution of Na⁺ between W1 and M. On the other hand, $E_{W2M, S}$, $E_{W2M, Rec}$ and $E_{W2M, rec}$ observed before the switch are mainly determined by the distribution of TEA⁺ between W2 and M. Accordingly, the value of $E_{W1-W2, Rec}$ ($E_{W1-W2, S}$ and $E_{W1M, rec}$) observed before the switch is estimated to be 0.35 V, and the experimental values observed before the switch from cell S to cell Ap or ap were about 0.37 V. Because the interfacial area of cell rec (or ap) is a quarter of that of cell Rec (or Ap), the magnitudes of the

limiting currents illustrated by i_{ap} and i_{rec} are equivalent to a quarter of those of the limiting currents (i_{Ap} and i_{Rec}) in Figs. 3 and 5.

The transfer of TEA⁺ from W1 to M is much easier than that of Na⁺ from W1 to M, since TEA⁺ is more hydrophobic than Na⁺.¹⁹ If the current due to the transfer of TEA⁺ from W1 to M is higher than the current due to the transfer of Na⁺ from M to W1, $E_{W1-W2, Rec}$ ($E_{W1-W2, rec}$) begins to shift in the negative direction. In addition, when the magnitude of the limiting current at the W1|M interface is higher than that at the W2|M interface, the potential-determining ion at the W1|M interface is changed from Na⁺ to TEA⁺.⁸ The potential balance in the electric circuit was lost by the switch. All interfacial potentials mutually varied to maintain the electroneutrality within all the phases. For example, $E_{W1-W2, Ap}$ was the potential difference between W1 and W2 through two routes of the electric circuit (W1(Ap)-M(Ap)-W2(Ap) and W1(Ap)-W1(Rec)-M(Rec)-W2(Rec)-W2(Ap)).⁸ The positive current (i) then flowed at the W1|M interface of cell Ap or ap, and the negative current ($-i$) simultaneously occurred at the W2|M interface of cell Ap or ap. In addition, the negative current ($-i$) passed at the W1|M interface of cell Rec or rec, and the positive current (i) occurred at the W2|M interface of cell Rec or rec. The current is determined by balancing the potential difference between two phases through one route with that through another route. In order to maintain the electroneutrality of all phases, the magnitudes of these currents were equivalent to each other. After switching of the connection, $E_{W1M, Ap}$ and $E_{W1M, ap}$ varied from -0.37 V to more negative potentials. Similarly, $E_{W1M, Rec}$ and $E_{W1M, rec}$ were shifted in the positive direction. When cell rec was connected to cell Ap, the shift of $E_{W1M, rec}$ was the highest. On the contrary, by switching the connection with cell Rec from cell S to cell ap, the shift of $E_{W2M, Rec}$ was the lowest. Thus, we have concluded that the propagation of the change in the membrane potential was caused by the generation of the circulating current within the membrane system. The results indicate that the existence of the threshold potential on the nerve transmission can be elucidated by the magnitude of the influx at the active site.¹⁻⁶ The reason why the nerve cell has a unique structure can be considered to be due to the circulating current.

The influence of the magnitude of the limiting current at the interface of the potential-sending site on the propagation of the change in the membrane potential

As previously described, the higher the ratio of the interfacial

area of the potential-sending cell to that of the potential-receiving cell, the more rapidly the change in the membrane potential is propagated. When the current density of the imaginary limiting current at the W1|M interface of cell ap is much higher than that at the W1|M interface of cell Rec, the membrane potential is quickly changed by the switching. When the concentration of TEA⁺ in W1 of cell ap was changed from 2×10^{-5} M to 10^{-3} M, the change in the membrane potential of cell Rec was higher than that observed before the addition of TEA⁺ to W1, as shown in Fig. 6(a). The $E_{W1-W2, Rec}$ value changed from 0.38 to 0.11 V even when cell ap was connected to cell Rec. Under the initial conditions, cell Rec was connected with cell S. The circulating current began to immediately flow by changing the switch from cell S to cell ap. Simultaneously, the membrane potential of cell Rec varied to the potential close to the action potential. The imaginary limiting current for the connection of cell ap to cell Rec in the presence of 10^{-3} M TEA⁺ was about 3.0 μ A which was about 40 times higher than that in the presence of 2×10^{-5} M TEA⁺. Thus, it was found that the propagation property depends on the magnitude of the imaginary limiting current within the potential window at the W1|M interface of the potential-sending cell. Accordingly, the propagation of the change in the membrane potential from the potential-sending cell to the potential-receiving cell is discussed by considering the magnitude of the imaginary limiting current flowing at the W1|M interface, as described below.

When the magnitude of the imaginary limiting current ($i_{lim, W1|M}$) observed within the potential window at the W1|M interface of the potential-sending cell (Ap and ap) is higher than 0 A, a change in the membrane potential occurs and begins to propagate.¹⁰ Accordingly, the magnitude of the imaginary limiting current at the W1|M interface of the potential-receiving cell (Rec and rec) corresponds to the threshold. In the present study, $i_{lim, W1|M}$ at the W1|M interface of the potential-sending cell ($i_{lim, W1|M}$ (ps)) can be approximately represented as Eq. (5).

$$i_{lim, W1|M} (ps) = kA (c_{TEA, W1} - c_{Na, M}), \quad (5)$$

where A is the interfacial area of the potential-sending cell, $c_{TEA, W1}$ is the concentration of TEA⁺ in W1, $c_{Na, M}$ is the concentration of Na⁺ in M, k is the coefficient concerning the diffusion coefficients, etc. The magnitude of $i_{lim, W1|M}$ (ps) can be regarded as a measure of the motive force to propagate the change in the membrane potential. Since the W2|M interface of each cell was depolarized by the transfer of TEA⁺, $E_{W2|M}$ of each cell slightly varied with the generation of the circulating current. On the other hand, $i_{lim, W1|M}$ at the W1|M interface of the potential-receiving cell ($i_{lim, W1|M}$ (pr)) can be described by Eq. (6).

$$i_{lim, W1|M} (pr) = -k'A'c_{Na, M}, \quad (6)$$

where A' is the interfacial area of the potential-receiving cell, $c_{Na, M}$ is the concentration of Na⁺ in M and k' is the coefficient like k . k' can then be presumed to be equal to k . Due to the fact that the magnitude of the circulating current in the steady state is almost equivalent to the magnitude of $i_{lim, W1|M}$ (pr), the magnitude of $i_{lim, W1|M}$ (pr) corresponds to the capacity for the circulating current to flow. When cells Ap, ap, Rec and rec are used, $i_{lim, W1|M}$ (pr) and $i_{lim, W1|M}$ (ps) are expressed by i_{Ap} , i_{ap} , i_{Rec} and i_{rec} , respectively. The ratio of $i_{lim, W1|M}$ (ps) to $i_{lim, W1|M}$ (pr) reflects the feasibility of the propagation of the change in the membrane potential.

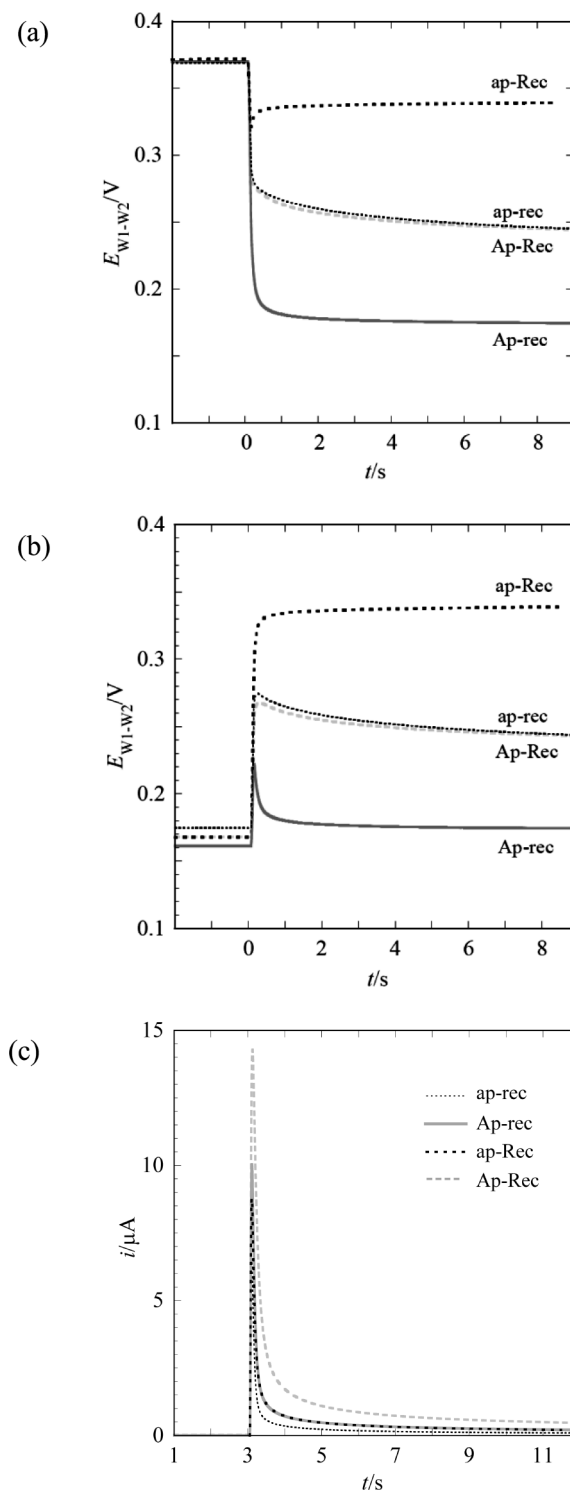


Fig. 4 The time-courses of the membrane potentials of the potential-receiving cells ($E_{W1-W2, Rec}$ or $E_{W1-W2, rec}$) by changing the connection with cell Rec (rec) from cell S to cell Ap (ap) (a), the potential differences of potential-sending cells ($E_{W1-W2, Ap}$ or $E_{W1-W2, ap}$) (b) and the circulating currents (i) (c). Curves 1: changing the connection with Rec from S to Ap, curves 2: changing the connection with rec from S to Ap, curve 3: changing the connection with Rec from S to ap, curve 4: changing the connection with rec from S to a. $t = 0$: the period of the switch. Interfacial area: 1.33 cm² (S, Ap and Rec), 0.331 cm² (ap and rec).

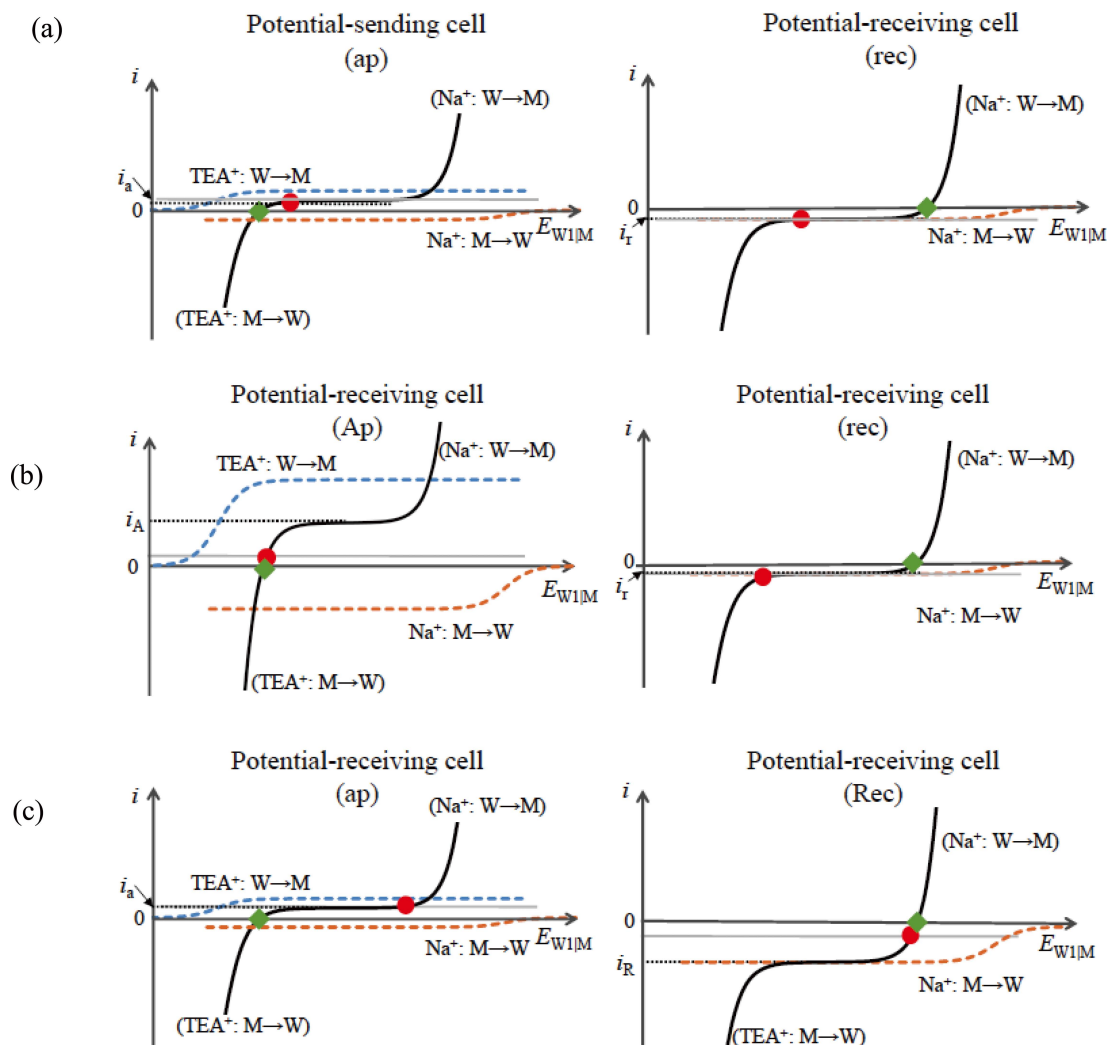


Fig. 5 Schematic steady-state voltammograms by considering the ionic composition and the ion transfer potentials of the ions at the interfaces of W1|M of cells ap and rec (a), W1|M of cells Ap and rec (b) and W1|M of cells ap and Rec (c).¹⁹ ◆: $E_{W1|M,Ap}$, $E_{W1|M,ap}$, $E_{W1|M,Rec}$ and $E_{W1|M,rec}$ observed before the switch, ●: $E_{W1|M,Ap}$, $E_{W1|M,ap}$, $E_{W1|M,Rec}$ and $E_{W1|M,rec}$ observed after the switch. Gray line: the circulating current. Interfacial area: 1.33 cm² (S, Ap and Rec), 0.331 cm² (ap and rec).

$$\frac{i_{Ap}}{i_{rec}} > \frac{i_{Ap}}{i_{Rec}} = \frac{i_{ap}}{i_{rec}} > \frac{i_{ap}}{i_{Rec}} \quad (7)$$

Conclusions

The higher the ratio, the more rapidly the change in the membrane potential propagates. This indicates that the propagation property depends on the magnitude of the current generated at the W1|M interface of the potential-sending cell. When two liquid-membrane cells have the same ion composition, it is easy for the cell with a larger interfacial area to propagate the change in the membrane potential. In actual nerve cells, such as Purkinje cells, pyramidal cells, stellate cells, *etc.*,¹ it is well-known that the area of a synapse of the nerve cell is still larger than that of the nodes of Ranvier in the axon or that of the axon terminals. Accordingly, this makes it easy for the nerve cell to propagate the change in the membrane potential to the axon terminal. Although the significance of the transmembrane current on the propagation of the action potential in the heart was reported by Gray *et al.*,¹⁶ this agreed with the result that the propagation of the change in the membrane potential is governed by the magnitude of the influx current at the potential-sending site.

In the present study, the relation between the propagation of the change in the membrane potential and the circulating current was investigated by combining multiple liquid-membrane cells. Since the change in the membrane potential is propagated by the generation of the circulating current, the propagation property is determined by the ratio of the limiting current at the potential-sending site to that at the potential-receiving cell. The limiting current observed at the interface, of which the potential difference varies in the potential-receiving cell and corresponds to the threshold, and the magnitude of the limiting current at the interface, of which the potential difference varies in the potential-sending cell, reflects the potency of the propagation of the action potential. The properties for the propagation of the change in the membrane potential depend on the ratio of the magnitude of the imaginary limiting current at the potential-sending cell versus that at the potential-receiving cell.

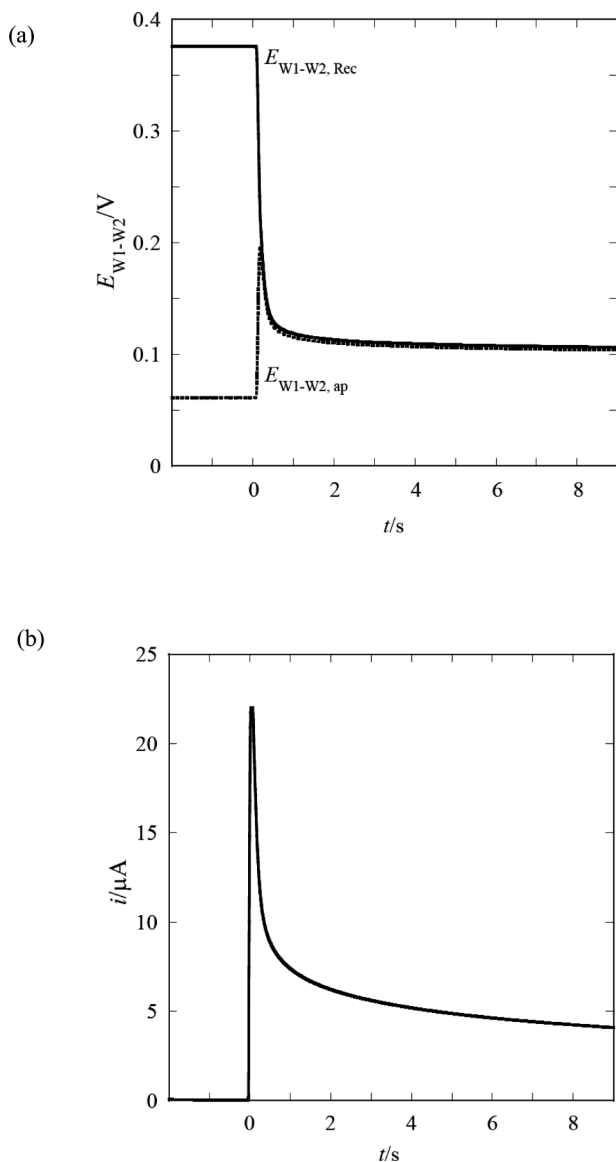


Fig. 6 Time-courses of the membrane potential of cells ap and Rec ($E_{W1-W2, ap}$ and $\Delta E_{W1-W2, Rec}$) (a) and of the circulating current (i) (b). Interfacial area: 1.33 cm² (S and Rec), 0.331 cm² (ap).

References

1. I. B. Levitan and L. K. Kaczmarek, "The Neuron: Cell and Molecular Biology, 3rd ed.", **2002**, Oxford University Press, New York.
2. R. Phillips, J. Kondev, and J. Theriot, "Physical Biology of the Cell", **2009**, Garland Science, New York.
3. W. Schwarz and J. Rettinger, "Foundations of Electrophysiology", **2000**, Shaker Verlag, Aachen, Germany.
4. F. Bretschneider and J. R. de Weille, "Introduction to Electrophysiological Methods and Instrumentation", **2006**, Elsevier, Amsterdam.
5. C. Egri and P. C. Ruben, "Action Potentials: Generation and Propagation", **2012**, eLS ©, John Wiley & Sons.
6. G. J. Kress and S. Mennerrick, *Neuroscience*, **2009**, *158*, 211.
7. S. Cullheim, *Neurosci. Lett.*, **1978**, *8*, 17.
8. N. Ueya, O. Shirai, Y. Kushida, S. Tsujimura, and K. Kano, *J. Electroanal. Chem.*, **2012**, *673*, 8.
9. Y. Kushida, O. Shirai, Y. Kitazumi, and K. Kano, *Bull. Chem. Soc. Jpn.*, **2014**, *87*, 110.
10. Y. Kushida, O. Shirai, Y. Kitazumi, and K. Kano, *Electroanalysis*, **2014**, *26*, 1858.
11. F. Offner, A. Weineerg, and G. Young, *Math. Biophys.*, **1940**, *2*, 89.
12. T. Tomita, *J. Theoret. Biol.*, **1966**, *12*, 216.
13. N. Maglaveras, F. Offner, F. J. L. van Capelle, M. A. Allesie, and A. V. Sahakian, *J. Electrocardiol.*, **1995**, *28*, 17.
14. N. Sperlakis and K. P. V. Murali, *Math. Comp. Model.*, **2003**, *37*, 1443.
15. D. Debanne, E. Campanac, A. Bialowas, E. Carlier, and G. Alcaraz, *Physiol. Rev.*, **2011**, *91*, 555.
16. R. A. Gray, D. N. Mashburn, V. Y. Sidorov, and J. P. Wilksw, *Biophys. J.*, **2013**, *104*, 268.
17. M. Delmar, D. C. Michaels, T. Johnson, and J. Jalife, *Circul. Res.*, **1987**, *60*, 780.
18. Y. Yoshida, M. Matsui, O. Shirai, K. Maeda, and S. Kihara, *Anal. Chim. Acta*, **1998**, *373*, 213.
19. Z. Samec, *Pure Appl. Chem.*, **2004**, *76*, 2147.
20. Y. Yoshida, Z. Yoshida, H. Aoyagi, K. Kitatsuji, A. Uehara, and S. Kihara, *Anal. Chim. Acta*, **2002**, *452*, 149.